Annals of Biomedical Engineering (© 2013)
DOI: 10.1007/s10439-013-0857-8

BMES BIOMEDICAL ENGINEERING SOCIETY™ www.bmes.org

Aortic Outflow Cannula Tip Design and Orientation Impacts Cerebral Perfusion During Pediatric Cardiopulmonary Bypass Procedures

PRAHLAD G. MENON,[1] JAMES F. ANTAKI,[1] AKIF UNDAR,[2] and KEREM PEKKAN[1]

[1]Department of Biomedical Engineering, Carnegie Mellon University, 700 Technology Drive, #4319, Pittsburgh, PA 15219, USA; and [2]Department of Pediatrics, Penn State Hershey College of Medicine, Hershey, PA, USA

(*Received 6 January 2013; accepted 24 June 2013*)

Associate Editor Ender A Finol oversaw the review of this article.

Abstract—Poor perfusion of the aortic arch is a suspected cause for peri- and post-operative neurological complications associated with cardiopulmonary bypass (CPB). High-speed jets from 8 to 10FR pediatric/neonatal cannulae delivering ~1 L/min of blood can accrue sub-lethal hemolytic damage while also subjecting the aorta to non-physiologic flow conditions that compromise cerebral perfusion. Therefore, we emphasize the importance of cannulation strategy and hypothesize engineering better CPB perfusion through a redesigned aortic cannula tip. This study employs computational fluid dynamics to investigate novel diffuser-tipped aortic cannulae for shape sensitivity to cerebral perfusion, in an *in silico* cross-clamped aortic arch model modeled with fixed outflow resistances. 17 parametrically altered configurations of an 8FR end-hole and several diffuser cone angled tips in combination with jet incidence angles toward or away from the head–neck vessels were studied. Experimental pressure-flow characterizations were also conducted on these cannula tip designs. An 8FR end-hole aortic cannula delivering 1 L/min along the transverse aortic arch was found to give rise to backflow from the brachicephalic artery (BCA), irrespective of angular orientation, for the chosen ascending aortic insertion location. Parametric alteration of the cannula tip to include a diffuser cone angle (tested up to 7°) eliminated BCA backflow for any tested angle of jet incidence. Experiments revealed that a 1 cm long 10° diffuser cone tip demonstrated the best pressure-flow performance improvement in contrast with either an end-hole tip or diffuser cone angles greater than 10°. Performance further improved when the diffuser was preceded by an expanded four-lobe swirl inducer attachment—a novel component. In conclusion, aortic cannula orientation is crucial in determining net head–neck perfusion but precise angulations and insertion-depths are difficult to achieve practically. Altering the cannula tip to include a diffuser cone angle has been shown for the first time to have potential in ensuring a net positive outflow at the BCA. Cannula insertion distanced from the BCA inlet may also avoid backflow owing to the Venturi effect, but the diffuser tipped cannula design presents a promising solution to mitigate this issue irrespective of *in vivo* cannula tip orientation.

Address correspondence to Kerem Pekkan, Department of Biomedical Engineering, Carnegie Mellon University, 700 Technology Drive, #4319, Pittsburgh, PA 15219, USA. Electronic mail: kpekkan@andrew.cmu.edu

INTRODUCTION

The arterial cannula has been shown to have a greater impact on regulating flow rate under continuous flow pumping conditions in a neonatal extracorporeal circulation than the venous cannula.[38] Further, large multi-center clinical studies have reported the association of a single arterial cannulation site to stroke risk and mortality post CPB circulatory arrest, in addition to other post-operative complications such as bleeding, renal or respiratory failure and sepsis.[39] This warrants specific attention to arterial perfusion in conjunction with improving peri- and post-operative CPB outcomes. Common arterial cannulation sites are located at the aorta, femoral, axillary or subclavian (with or without a side graft), external iliac, and innominate artery. Arterial perfusion by cannulation of the ascending aorta is regarded as an important advance in cardiovascular surgery and is the focus of this study since the technique eliminates the issues of retrograde aortic perfusion[21] and the need for a second incision for femoral cannulation during CPB. The aortic cannula must ideally be placed high up in the ascending aorta[10] but improper technique can occasionally result in profuse bleeding as a result of improper cannula placement. To date, CPB has been studied in regard to clinical stroke-risk,[2] but there have been few reported studies of the detailed fluid dynamics associated with aortic cannulation,[15,16,31,40] all underscoring the association of biomechanical risks with aortic cannulation. Despite advances in surgical

Published online: 02 July 2013

techniques leading to decreased mortality after repair of complex congenital cardiac conditions, neurologic morbility is still significant. Given that the incidence of neurological morbidity is as high as 30% in infants and children[8,37] undergoing CPB in sharp contrast with 2–5% amongst adults, the issue of aortic perfusion during CPB deserves attention in young patients.

The conventional principle for characterizing arterial cannula devices has been based on driving pressure drop vs. outflow rate characteristics[26] studied from *in vitro* experiments.[6,38] Pressure-flow characteristics in general become increasingly unfavorable at reduced outflow diameters, for conventional end-hole type standard aortic outflow cannula configurations. Post intervention recovery has been reported to be suboptimal[24,34,41] and unless better aortic cannulation techniques are developed, the incidence of cannula-related problems can be expected to grow in proportion to the increased utilization of cardiopulmonary bypass (CPB) procedures or continuous-flow pediatric blood pumps. Poor perfusion of the aortic arch is hypothesized as a cause for neurological complications which may attribute to increased stroke risk on account of dislodged emboli transported in a non-physiologic flow field created by a single high speed cannula jet. Our previous numerical and experimental studies in a cuboidal test-rig setup[25] have demonstrated that an efficient aortic outflow cannula tip design can make a difference in allowing higher blood volume flow rates at low exit force, which can potentially mitigate intimal vascular damage and shear related blood damage risks. This suggests that in addition to cannulation strategy, cannula tip design can improve the practice of aortic cannulation.

Apart from preordained extra-operative cannula design and determination of device deployment, intra-operative monitoring of their performance *viz*. cannula outflow velocity, pressure gradients and real-time aortic flow distributions—would be of great value. However, today we are limited in the availability of accurate, reproducible and noninvasive imaging modalities to achieve this feat satisfactorily in the entire aortic arch during CPB. While phase contrast MRI (PC-MRI)[4] can be employed to examine physiological flow conditions in larger vessels either pre- or post-operatively, it cannot be used intra-operatively. Further, although transcranial Doppler Ultrasound[36] is a sensitive, real time tool for monitoring cerebral blood flow velocity which is employed intra-operatively it has a relatively small field of view for velocity measurement is difficult to span the entire aortic arch and limits precise intra-operative monitoring of pressures during CPB. This again emphasizes the importance for numerical modeling in the cannulated aortic arch, in order to adjudge the quality of perfusion during CPB. Recent studies in regard to neonatal aortic cannula design have suggested that engineering better device-specific jet flows[25] through a re-engineered cannula tip may have an impact on improved hemodynamics and reduced sub-lethal hemolytic damage. In this study, we move one step closer to identifying parameters of importance in designing novel aortic cannula tips for use in a neonatal aortic arch that satisfy the prevailing emphasis on favorable pressure-flow characteristics (i.e., lower M-numbers[26]) while also paying attention to sensitivity of the tip design on perfusion to the head–neck vessels of the aortic arch, during CPB. Our goal is therefore to extend both the design rationale and the relevance of having a diffuser cannula tip—an improvement to the standard end-hole tip design—presenting not only decreased blood damage and increased permissible flow rates, as indicated from our previous studies[25] but by additionally examining aortic perfusion in an *in silico* CFD setting.

Finally, to-date, although fluid dynamic design of blood handling devices,[3,43,44] stents,[11] vascular grafts[7] and heart valves[1] have been studied using coupled CFD shape optimization methodologies, the application of this paradigm to fully three-dimensional (3D) parametric shape sensitivity analysis of hemodynamics during aortic cannulation has been found wanting. Therefore, a coupled CFD shape sensitivity analysis is presented in this study for the first time in relation to the cannula tip, focusing efforts toward a diffuser tip design.

METHODS

This study was divided into several stages in order to first establish the importance of aortic cannula tip design on outflow hemodynamics and then to examine the effects of cannula tip design and orientation on perfusion to the great vessel branches of the aortic arch providing cerebral perfusion. The improvements proposed by way of the novel cannula designs evaluated in this study relate to the internal flow-control for effectively decreasing jet velocity while reducing wall-shear stress within in the cannula, and mitigating early onset of turbulent unsteadiness in the jet wake. For specific application to neonatal and pediatric CPB perfusion, design considerations included having a small inner diameter of cannula (2 mm) to minimize disruption of the aorta; a diffuser tip hypothesized to improve pressure-drop vs. flow-rate characteristics and reduces exit force (and outflow velocity); and a diverging and then converging four-lobe swirl inducer responsible for reducing the wall shear stress (WSS) experienced by the blood in the device and also simultaneously improving vorticity of the coherent jet core in order to propel flow forward in a manner delaying the separation of flow in the diffuser cone. Use of a diffuser cone angle tip has

already been shown in previous studies to create vastly different jet flow characteristics than an end-hole tip with significantly diminished normalized index of hemolysis blood damage for a range of physiologically relevant flow regimes.[25] In this regard, three novel design features of hemodynamically superior aortic cannulae are presented (see Fig. 1, i–iii), each designed to delay onset of turbulence in the cannula jet wake, while simultaneously reducing exit force of the jet, for minimizing risk of intimal vascular injury, and improving outflow rate vs. driving pressure drop perfusion characteristics. This study additionally examines the merit of the diffuser tip's potentially significant role in improving head–neck perfusion in the aortic arch, which has not been previously investigated.

The methods have been organized as follows: First, "Cuboidal Test-Rig Simulations—An Initial Test of Cannula Tip Impact on Outflow" section describes, a direct numerical simulation (DNS) CFD employed in order to study the internal flow and device-specific jet flows hemodynamics of three cannula tip designs—end-hole, diffuser tip and diffuser tip preceded with four-lobe swirl inducer—in cuboidal test rig. Next, in "Flow Visualization and Pressure-Flow Experiments—Visual Corroboration of Numerical Results" section defines experimental methods for corroborating the observations from numerical experiments using high-speed dye flow visualization studies comparing cannula tip designs visually for their outflow jets, while also establishing the independent role of each component in the proposed cannula design modification. Device-specific pressure-flow characteristics are also evaluated. Finally "Aortic Arch Simulations with Resistance Boundary Conditions" and "Shape Sensitivity Objective Functions" sections define a shape-sensitivity analysis strategy to further discover the utility of the diffuser tip design in a cannulated neonatal aortic arch model, and examine the role of tip geometry and orientation on aortic head–neck vessel perfusion. The issue of cerebral hypoperfusion during CPB is addressed by first modeling the jet flows emanating from an end-hole cannula tip in a standard initial aortic cannulation orientation and insertion site, following which sensitivity of altered cannula tip-design and orientation on head–neck perfusion is studied by coupling CFD with a mesh-morphing based parametric shape alteration paradigm.

Cuboidal Test-Rig Simulations—An Initial Test of Cannula Tip Impact on Outflow

DNS CFD is first used to examine internal hemodynamics and the early developing cannula jet region and compare a conventional end-hole cannula tip jet against a diffuser cone tip designed to decelerate flow with and without a four-lobe swirl inducer preceding it (see Fig. 1). The swirl inducer is defined in terms of its four-lobed chamber design *viz.* the depth of the grooves of these four lobes and the pitch of the helical grooves. In this study, the utility of the swirl inducer is demonstrated in regard to its potential benefit for improved cannula hemodynamics using the two specific design features shown in Fig. 1. The design rationale for the swirl-inducer is to delay near-wall flow reversal (i.e., separation flow) effects of the proposed diffuser tip design. The diffuser tip is defined by the half-angle of the conical tip, θ (see Fig. 2c), which is examined in greater detail using a shape-coupled CFD approach in the latter half of this study. Novel designs tested in this section were composed of an elongated tube (inner diameter, $D = 2$ mm) having at least one of the following improvements: (a) a 1.0 cm long 7° diffuser cone tip with 2 mm inner diameter, D (Fig. 1, i); and (b) a four-lobe swirl inducer chamber (one complete 360° swirl over a 50 mm pitch), first diverging to 2.25D

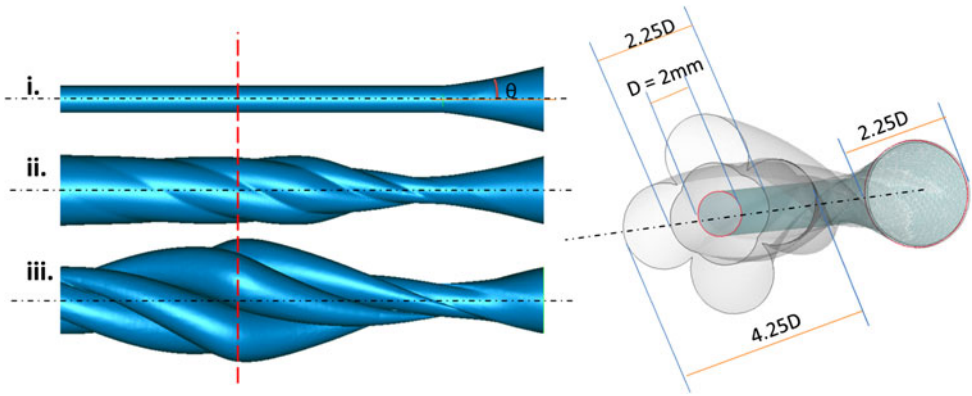

FIGURE 1. Left: Side profile views of three novel embodiments of 8FR cannula tips ending with a 7° diffuser cone tip. The two four-lobe swirl inducer design embodiments are depicted with differently sized lobe geometries. Right: The cross sectional shapes of the three cannula tip designs (arranged concentrically) depicted on the left have been demonstrated on the right in an isometric view clipped through the middle (i.e., at red-line on left).

and then converging to meet the inlet of a 1 cm long 7° diffuser cone tip having inlet diameter, D (Fig. 1, ii). For numerical flow testing in the cuboidal test-rig, a 7° diffuser was chosen as a feasible test model on account of preliminary dye flow visualization studies (not shown) which indicated an oscillating jet for large cone angles.

A second-order finite difference artificial compressibility solver[22,33,35] was employed for this section of the methods to numerically model the jet flows in a cuboidal test rig, in a manner similar to that conducted in previous studies.[25] The simulations in this section involved at least 1.5 M fluid nodes with a length scale discretization of ~0.03 mm and simulation time resolution of $O(10^{-5})$ s. Incompressible and Newtonian blood flow with constant hemodynamic properties ($\rho = 1060$ kg/m^3, $\mu = 3.71 \times 10^{-3}$ Pa s) was simulated with no-slip boundary conditions enforced at confining walls, which were assumed rigid and impermeable. 3D unsteady fluid dynamics of the confined jet streams was modeled at steady inflow rates corresponding to a Reynolds number (Re) of 1780 (~0.6 L/min). The studies described in this section were conducted in the Blacklight shared-memory supercomputing cyberarchitecture of the Pittsburgh Supercomputing Center, in parallel on 32 cores consuming up to 48 h per run.

Flow Visualization and Pressure-Flow Experiments—Visual Corroboration of Numerical Results

In order to further visually assess effects of the proposed cannula tip design improvements, dye flow visualization experiments were conducted to observe separation of flow past the cannula outlet and coherence of the resulting jet from different embodiments of the proposed diffuser tip, under steady physiological cannulation flow rates corresponding to Re 1780. A cuboidal test-rig developed for experimental testing of cannula jets[25] is employed in order to evaluate novel prototype cannula tip designs. Geometries were modeled in Pro-Engineer (Parametric Technology Corp., Needham, MA) and saved in STL format, whereupon they were prototyped by 3-D printer (Perfactory Mini, EnvisionTec, Dearborn, MI) at a resolution of ~25 μm and a build height of 50 μm. To accentuate the swirl inducing properties of the four-lobe swirl inducer design described in "Cuboidal Test-Rig Simulations—An

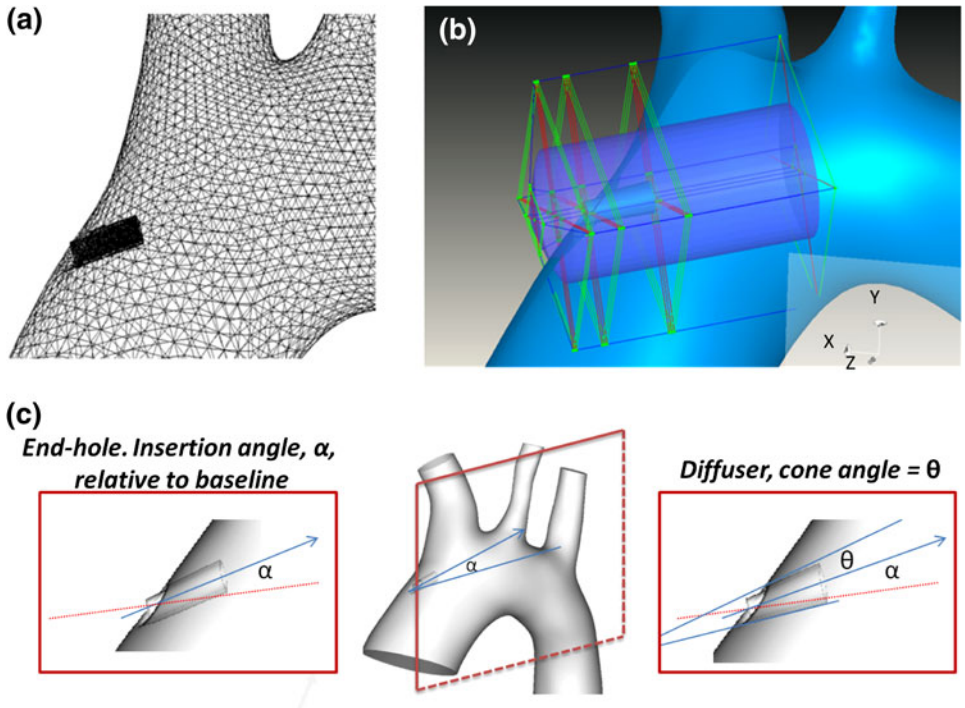

FIGURE 2. (a) Unstructured finite volume mesh as seen on the 8FR cannulated aortic arch walls indicating local refinement at the cannula inlet regions and the aortic outlets. (b) The ASD control volume (dark blue, right) used to morph the volume mesh while making adjustments to the aortic cannula tip orientation angle (toward or away from the head–neck branches, in the *X–Y* plane) and diffuser cone angle, in the Sculptor software program. (c) Parameters employed for shape sensitivity studies are illustrated, along with two sample cannulation configurations: α is the insertion angle subtended with the baseline insertion orientation (red dotted line) defined on the X–Y plane; and θ is the half-angle of the diffuser cone tip.

Initial Test of Cannula Tip Impact on Outflow" section (Fig. 1, ii) the experimentally tested design had an expanded divergent-convergent four-lobe swirl inducer chamber (see Fig. 1, iii) with deeper swirl lobes (one complete 360° swirl over a 50 mm pitch) having an outer diameter 4.25 times the rated cannula inner diameter, D, followed by a 1.0 cm long 7° diffuser cone tip. In order to isolate the jet wake in these visualizations, the mean image captured before the entry of the jet into the chamber was mathematically subtracted away from each frame of the high-speed video of the developing jet wake using a simple MATLAB image-processing routine.

In addition to the flow visualization setup, a second *in vitro* flow loop was employed to characterize jet axial pressure-flow characteristics (shown in Fig. 6a). Jet axial pressure measurements were obtained 70 mm downstream of the cannula inlet and at the immediately downstream of the submersible pump, using TruWave disposable pressure transducers (Edwards Life Sciences, Irvine, CA, USA). In order to identify the contributions of the diffuser to improved jet dynamics, pressure measurements were made for a range of flow rates for a rapid-prototyped models of 5°, 10° and 15° diffuser cone tips, with 0.5 or 1.0 cm each having cone inlet diameter of 2 mm, at identical flow conditions.

Aortic Arch Simulations with Resistance Boundary Conditions

Having established the fact that minor alterations to cannula tip design lead to tangible variability in the flow field from the DNS cuboidal test rig simulations (see "Cuboidal Test Rig" section), the next goal was to examine the effect of cannula tip geometry and orientation on aortic head–neck perfusion. It has been shown that stenoses or occlusions in the great vessels lead to altered flow direction in the vertebral arteries (seen on vertebral sonograms).[12] Therefore, reversal of flow in one of these great vessel branches may be expected to have similar effects in altering cerebral perfusion during CPB. To study the possible occurrence of flow reversals in the head–neck vessel branches, numerical simulation of different cannula designs placed in a clamped aorta was conducted. The vessel model for the aortic arch in these simulations were created from magnetic resonance angiography (MRA) reconstructions of a neonatal aortic arch[25] which was cannulated by *in silico* parametrically insertion of a cannula tip into the ascending aorta after cross-clamping it.

Three-dimensional CFD models of blood flow inside the cross-clamped aortic arch were conducted to compare the flow characteristics of several cannulae designs created by morphing an initial cannula design (end-hole, straight tip) in a pre-defined baseline orientation (Fig. 2) into different configurations. Given the aorta's helically twisted transverse shape, surgeons prefer to insert the cannula straight along the transverse arch direction. This orientation was considered as an initial cannulation position (see Fig. 2, left) which in-turn was parametrically altered to create a range of cannula tip configurations. A set of 17 tip configurations was automatically populated by altering both tip conical angle and outflow orientation using an algorithm defining an optimal Latin hypercube design of experiments,[32] implemented in the Sculptor software package (Optimal Solutions Software, LLC, Idaho Falls, ID) for optimal designs for computer experiments based on a set of predefined parameters.

The parameters chosen for cannula insertion included cannula insertion angle, α, and cannula tip diffuser cone angle, θ, with the zero cone angle being the limiting case of an end-hole design. Insertion depth and location of incision were maintained constant (see Fig. 2). Traditionally, such parametric design alterations would require the time-consuming process of regenerating a new geometry and CFD mesh for each new cannula orientation. However, in this study, a commercial meshing morphing tool, implemented in the Sculptor software, was employed to deform the shape of the cannula tip parametrically using arbitrary shape deformation (ASD) technology for smooth volumetric shape deformations, based on movements of user-defined control points. A cylindrical ASD volume (Fig. 2, right) was employed for maximum control over mesh deformation of the axis-symmetric tip geometries and reduced likelihood of negative mesh volumes after deformation.

Three-dimensional unsteady CFD simulations were conducted in a cross-clamped aortic perfusion during CPB, under 1 L/min (~Re 2150) steady cannulation flow, assuming continuous flow blood pumping from the extracorporeal circuit. The simulations described this section were conducted in commercial software, Fluent (ANSYS Inc, Cannonsburg, PA), using a second order accurate PISO finite volume numerical discretization for pressure and velocity to solver the unsteady incompressible Navier–Stokes equations. The non-uniform unstructured finite volume mesh was generated with tetrahedral elements (~100,000 fluid elements) in Gambit (ANSYS Inc., Cannonsburg, PA) with finer elements in the head–neck vessels and near the cannula tip (see Fig. 2). Adaptive time-stepping was considered in order to favor better solution convergence and instantaneous flow field data was analyzed at the after one second of flow.

Mesh sensitivity analysis was performed for the un-morphed original meshed geometry (i.e., end-hole cannula in standard orientation), by examining convergence of the head–neck outflow distributions

achieved to within 5% of mass flow at each outlet, to ensure the consistency of the baseline case. Since mesh morphing was applied to the cannula tip region, the cannula region was adaptively refined to a higher density by adjusting the number of nodes along an edge length during meshing, in order to both improve the quality of flow physics in the region and to avoid negative or highly skewed volumes resulting from mesh morphing. Hence, all simulations had the same mesh configuration, although morphed at the cannula region. This approach helped ensure that the flow results from the different cannula orientation cases in our optimal Latin hypercube of experiments were comparable to the best possible extent.

Incompressible and Newtonian blood flow modeling with constant hemodynamic properties ($\rho = 1060$ kg/m^3, $\mu = 3.71 \times 10^{-3}$ Pa s) was employed and no-slip boundary conditions were enforced at confining vessel walls and the aortic cross clamp, which were assumed rigid and impermeable. Head–neck outlets were modeled using a constant outflow resistance equation which regulated cerebral blood flow and pressure at the outlets to the aortic arch, while preserving flow continuity (converged to within $O(10^{-4})$). The constant outflow resistances, R_i, applied at an outlet, i, was used to iteratively update pressure, P_n, at an outlet based upon the net outflow rate, Q_i, after each iteration, for steady cannulation conditions. A relaxation parameter, α, was employed during outlet pressure correction to ensure stability of the solution ($\alpha < 1.0$). This was achieved in the following simple two-step procedure:

$$P_i = Q_i R_i + P_0 \tag{1}$$

$$P_i = \alpha(P_i - P_n), \tag{2}$$

where P_0 is the operating pressure which was set at 5 mmHg simulative of central venous pressure. Equation (2) defines a relaxation approach to help with simulation convergence while iteratively adjusting the pressure at the aortic outlets in order to achieve the eventual outflow distributions characteristic of a given aortic cannula configuration. The flow-independent vascular resistances applied at outflow boundaries of the neonatal aortic arch model were tuned such that they ensured a head–neck outflow split of 40% at steady cannulation flow using the baseline end-hole cannula. Resistances of the individual head–neck vessels were set relative to each other as per Poiseuille equation i.e., vascular resistance is inversely related to the fourth power of outlet diameter.

Note that the goal of the Fluent CFD coupled shape-sensitivity simulation approach described in this section was less to examine local flow structures at the cannula tip but rather to determine the head–neck vessel flow distribution resulting from different cannula orientations. But although the mesh resolution chosen for this shape-sensitivity analysis was lower in spatial resolution in comparison with the DNS cuboidal test-rig simulations (in "Cuboidal Test-Rig Simulations—An Initial Test of Cannula Tip Impact on Outflow" section), spatiotemporal resolution was sufficient to observe similar major flow structures and developing jet-axial velocity profiles as that seen in the cannula jets tested in the cuboidal test rig. The shape-sensitivity analysis in this section were conducted in parallel on a 8-core Intel Xeon processor with 8 GB of RAM and consumed approximately an hour per CFD run.

Shape Sensitivity Objective Functions

Cerebral perfusion is a fraction of the flow leaving the aortic head–neck vessels, accounting for the flow diverted into the subclavian arteries. Normal cerebral blood flow i.e., the total of flow through the left and right vertebral and internal carotid arteries, accounts for 22–25% of the cardiac output in neonates and 15% (~850 mL/min) in adults. The proportion of cerebral perfusion to cardiac output is higher in the case of neonates and therefore, it is of utmost importance to ensure continuous positive outflow into the great vessel branches. Given that cerebral perfusion is a fraction of the flow out the aortic head–neck vessels, an objective function considering maximization of perfusion to the head–neck vessels of the aortic arch i.e., minimizing flow to the descending aorta (DAo), was computed as an index of efficiency of cerebral perfusion. The two specific functions analyzed for shape-sensitivity were: (1) percentage DAo mass flow split; and (2) mass flow at the brachicephalic artery (BCA).

Perfusion in the great vessels as a result of geometric changes was collected for each case from the instantaneous flow field after 1 s of flow. The result of analysis was finally rendered using as a surface plot defining the objective function vs. the two independent parameters considered in this study *viz*. diffuser half-cone angle and insertion angle orientation change. The shape-sensitivity surface plots were prepared by applying a simple-krigging operation onto the data resulting from simulations and effectively define the shape-sensitivity of cannula tip configuration on head–neck perfusion.

RESULTS

Cuboidal Test Rig

As an initial examination of the cannula jet, the instantaneous shear layer surrounding the irrotational

jet core was visualized using flow streamlines in the near-outlet region (Fig. 3a), and the velocity field in the early jet region (Fig. 4). The computationally tested embodiment of the swirl inducer with diffuser tip (see Fig. 1, ii), revealed four coherent vortical structures created by each of the four lobes of the swirl-inducer, which were visible distinctly through visualization of 3D vorticity and helicity isocontours (Figs. 3b and 3c). The temporal unsteadiness in the jet was noted 0.03 s into jet development were found to be tangibly reduced by virtue of the four-lobe swirl chamber (Fig. 4) in comparison with a standard end-hole cannula of the same inner diameter as well as one with a 7° diffuser cone tip but without a swirl inducer. This supports the initial hypothesis that the swirl inducer presents an internal flow-control feature for increased permissible flow rate and pressure-flow characteristics in combination with the diffuser tip design, delaying the onset of flow separation and complex jet wake turbulence at physiological CPB flow rates; facilitating a more coherent jet stream at high speeds.

Dye Flow Visualization

In order to identify the individual contributions of the diffuser and the swirl inducer to the improved jet dynamics, component-wise function (Figs. 5a–5c) of the diffuser and swirl-inducer regions was studied individually by dye flow visualization. The novel swirl-inducing design that was experimentally tested had more pronounced internal flow control features (see Fig. 1, iii), featuring a greater expanded region (4.25*D*) than the version tested in the cuboidal chamber using CFD. The swirl inducer encompassed one full 360° twist along its length in order to rotate the incoming fluid by a greater angle during its linear travel. Increased expansion at the swirl inducer enhanced swirling flow, reduces mean flow velocity in the swirl chamber and is likely to reduce fluid induced shear

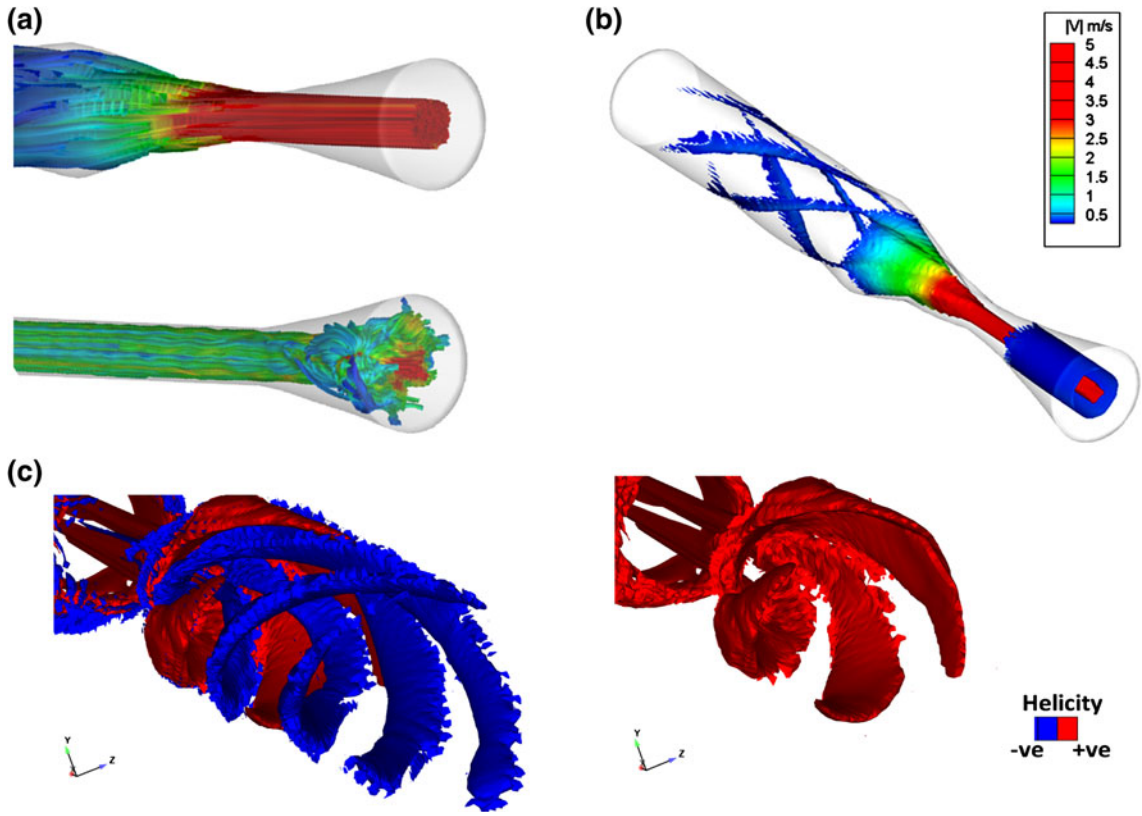

FIGURE 3. (a) Flow streamlines colored by velocity in test cases of an 8FR (~2 mm) cannula integrated with a 7° diffuser cone (*Re* 1780 at diffuser inlet) are presented i.e., preceded with (above) and without (below) a four-lobe swirl inducer chamber. A tight coherent jet core is created as the swirl chamber converges down to the diameter of the diffuser inlet. Jet temporal unsteadiness at the diffuser cone is tangibly reduced by virtue of the swirl chamber. (b) The tested swirl inducer (shown in Fig. 1, ii) was three times the diameter of the cannula body and is associated with four coherent vortical structures matching the lobes of the swirl inducer, as highlighted by the vorticity isosurfaces. (c) Isosurfaces highlighting positive and negative helicity of vortical structures in the swirl inducer lobes better define the rotation about the vortex cores shown in (b).

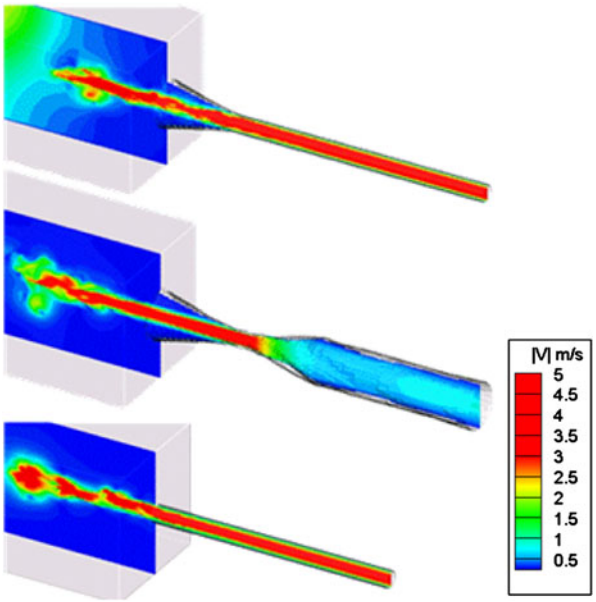

FIGURE 4. Comparison of three cannula jets all having a minimum diameter of 2 mm, observed at 0.03 s from jet initiation (*Re* 1780). The swirl inducer cannula tip (middle—shown in Fig. 1, ii) has a distinctly more coherent jet than the end-hole tip's complex unsteady/dissipating jet wake (top). The diffuser tip jet (bottom) is marginally more coherent than the end-hole jet but had a shorter potential core length and experienced earlier flow separation in the diffuser cone than the version preceded with a swirl inducer.

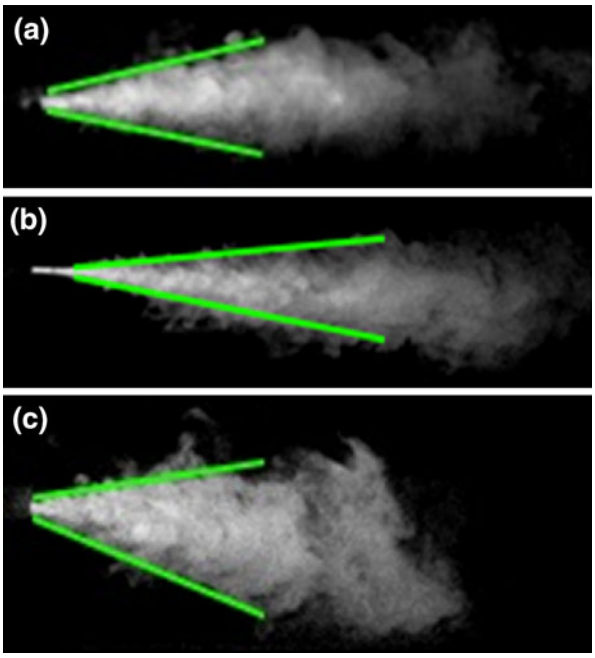

FIGURE 5. (a) Dye flow visualization of the four-lobe swirl-inducer plus 7° diffuser tip cannula shown in Fig. 1, iii. (b, c) The individual component-wise function of the swirl-inducer (b) and diffuser (c) regions of the novel cannula design, The swirl inducer led to a more coherent tighter jet, as demonstrated from DNS CFD simulations, while the diffuser component reduced outflow velocity while increasing the diverging cone-angle of the jet.

stress inside the device. Despite its higher exit velocity, the end-hole tip jet as visible by means of the diffusive dye front was noted to propagate axially at a slower rate in the early developing jet region (close to the inlet) due to the highly dissipative nature of the developing end-hole jet owing to its turbulent characteristics, in contrast with the jets from the novel diffuser tip design embodiments equipped with swirl inducers which exhibited diffusive dye fronts propagating forward more rapidly owing to less dissipation in the developing jet region.

The Coanda effect i.e., the property of a jet stream to adhere to the boundary wall, was observable from the dye flow visualizations in 1 cm long diffuser cone angles exceeding 10° (not shown). This effect manifested itself by way of a periodic oscillation in the jet stream which became more pronounced at high diffuser angles. Dye flow visualization conducted on a 1.0 cm long 7° diffuser tip in contrast with a 2.0 cm long one revealed that the Coanda effect was more pronounced for a longer diffuser length, indicating a potentially a limiting length for diffuser tip. This effect may possibly be mitigated until longer diffuser tip lengths with a stronger swirl inducer preceding the tip. The dye-flow visualization experiments confirmed that size and prominence of the swirl inducer grooves are important factors in contributing to improved coherence of the outlet jet at high speeds.

Experimental Analysis of Diffuser Angle Sensitivity to Pressure-Flow Characteristics

The experimental setup employed for pressure-flow measurements along the jet axial length is shown in Fig. 6a. Analysis of static pressures downstream of the end-hole and diffuser cone jets revealed that the diffuser showed significantly positive static pressure values 70 mm axially downstream of the jet inlet, in comparison with an equivalent end-hole cannula, indicating a softer outflow jet i.e., lower exit force and outflow velocity. Several diffuser cone angles were analyzed to arrive at an optimal diffuser cone angle. Figure 6b shows the pressure drop vs. flow rate relationship for an end-hole and several diffuser tips, along the jet axis. The end-hole cannula tip required a significantly higher driving pressure from the pump in order to propel axially forward, in comparison with the diffuser cone cannula tip. This analysis suggests that the diffuser not only provides desirable jet flow characteristics, as has been discussed by virtue of its potential core length, velocity field and blood damage analyzed in previous studies,[25] but simultaneously also has desirable pressure-flow characteristics which can reduce the requirement of pumping pressures in the

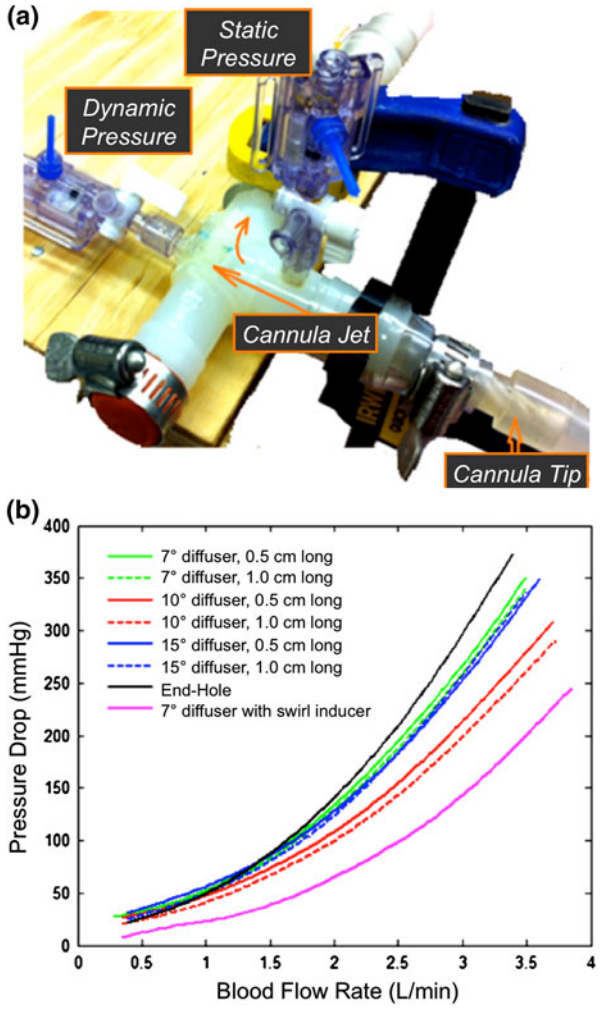

FIGURE 6. (a) Experimental setup for characterizing pressure drop vs. flow rate relationships in several diffuser tipped cannulae (8FR inlet inner diameter, ID) and the one 7° diffuser tip preceded by the four-lobe swirl inducer tested in dye-flow visualization studies (magenta line—cannula iii in Fig. 1). (b) Pressure-flow characteristics measured along the cannula jet-axis are compared against a standard 8FR ID end-hole cannula (black line). Flow rate was dynamically scaled to that of blood, based on *Re*. Pressure drop is for 70 mm section along the jet axis. Inner diameter is 2 mm for all cases.

extracorporeal circulation circuit during CPB procedures.

Lower downstream static pressures were noted for the swirl inducer jet without the diffuser therefore indicating that it is likely to have undesirably high outflow speeds for the same flow rates, at the cost of higher driving pressure gradient from the pump. The cost of greater exit force is may translate in likely intimal vascular damage to the aorta. The addition of the diffuser clearly reduced the exit force of the swirl inducer jet, as was verified by the higher (more positive) values of static pressure observed 70 mm axially downstream. The diffuser also allowed the jet to propagate axially with lesser driving pressure from the pump. The end-hole tip required a greater pump driving pressure in order to propel the same volume of fluid axially forward, in comparison with the swirl-induced jets.

In Silico Sensitivity of Diffuser Angle and Insertion Orientation on Head–Neck perfusion

In an ideal use case or mode of operation, the cannula blood jet (typically *Re* 650–2150) exits along the direction of the transverse aortic arch, heading towards the curvature of the DAo, in a manner that mitigates high-speed jet impingement on the walls of head-and-neck vessel branches, minimizing stroke risk due to dislodged thrombi from the mechanical circulatory support systems. The straight end-hole jet elicited a large reaction on the aortic wall (see red in Fig. 7, left) as evidenced by higher WSS, presenting a threat of diverting emboli from the clamp region or the extra-corporeal circulation into the head–neck vessels. WSS in the end-hole case was uniformly higher throughout the transverse arch, most pronounced at the location of jet impingement and up to ten times higher than the physiologic time-averaged WSS expected physiologically in an aorta.[27] This high WSS carried forward through the aortic isthmus due to the high velocity of the outflow jet streamlining along the DAo. WSS in the diffuser tip cases were markedly lower at the aortic isthmus and DAo, including at the region of jet impingement due to the reduced outflow jet speed of the diffuser tip (see Fig. 7b).

Shape sensitivity analysis was conducted with the goal of seeking monotonicity between the decision variables. The tested cannula tip configurations filled an optimal Latin Hypercube of design experiments defining the response for cerebral perfusion as a function of input parameters (see Fig. 2c): (a) cannula insertion angle, α—defined relative to an initial feasible cannulation angle, positive in the direction of head and neck vessels; and (b) diffuser cone angle of cannula tip, θ. The BCA was noticed to experience backflow, given the set resistance outflow conditions, if either the cannula jet was directed straight toward the left common carotid artery (LCCA) or left subclavian artery (LSCA), or when angled directly toward the junction between LCCA, BCA or LCCA, LSCA. While the orientation of the end-hole cannula toward the head and neck vessels improved net volume of flow towards the head and neck, it did not solve the problem of backflow at the BCA. The anticipated alteration in flow direction at the vertebral arteries as a result of a BCA backflow event has been illustrated in Fig. 8.[12] However, cerebral

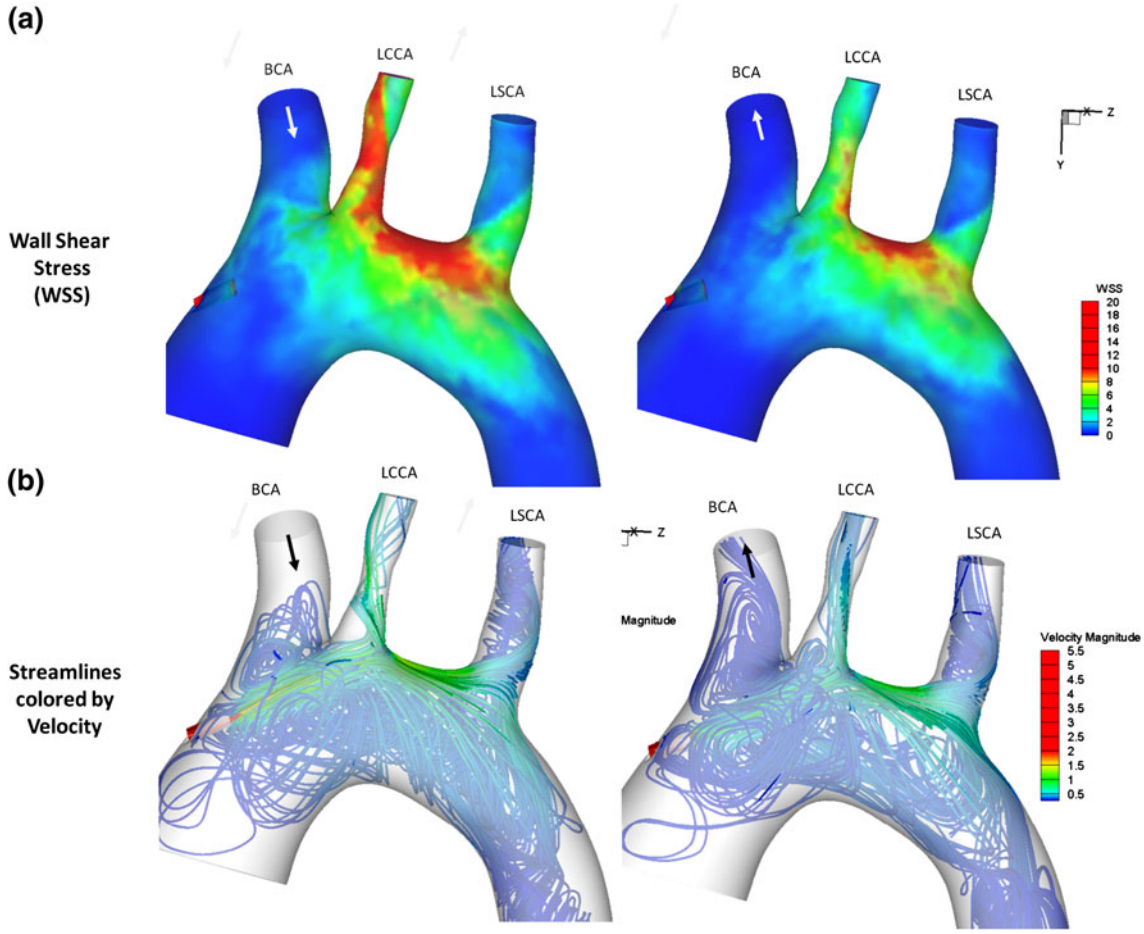

FIGURE 7. Comparison between: (a) WSS; and (b) streamlines colored by velocity magnitude; in two *in vivo* cannulation configurations considered in the optimal Latin hypercube *viz.* the end-hole cannula angled toward the head–neck vessels (left) and a $\theta = 7°$ diffuser tipped cannula inserted the same angle, α (see Fig. 2 for definitions of θ, α). BCA backflow was observed for the end-hole tip (left). The diffuser (right) markedly reduced backflow issues and outflow velocity for the same cannulation flow rate. The illustrated diffuser tip angled toward the head–neck vessels (right) had the best head–neck perfusion ratio for the set resistance outflow boundary conditions in the test neonatal arch and had reduced peak and mean WSS in the aortic arch in contrast with an end-hole cannula. BCA: brachicephalic artery; LCCA: left common carotid artery; LSCA: left subclavian artery.

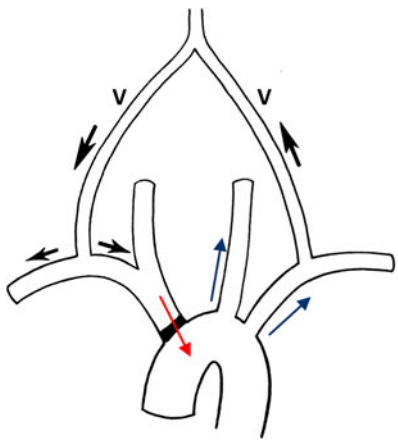

FIGURE 8. The flow directions expected in the vertebral arteries (labeled: V) as a result of non-physiologic BCA flow direction (red: occlusion or backflow) distinctly indicates a situation with compromised cerebral blood flow in this configuration.[12] BCA: brachicephalic artery.

perfusion was noted to improve with diffuser tip angle, irrespective of the cannulation orientation angle. The 7° diffuser cannula angled toward the BCA had the best head–neck perfusion ratio (see Fig. 7, right) with ~50% of flow diverted to the head–neck vessels for the modeled outflow resistance conditions in contrast with ~40% at the initial position with an end-hole tip.

The shape sensitivity CFD studies conducted on the 17 cannula tip configurations revealed important effects on head-and-neck mass flow distribution and are summarized as simple-krigging surface plots in Fig. 8. Generally, the closer the jet was angled toward the base of the BCA, the greater was the extent of backflow observed (blue regions on Fig. 9b). This is expected as a result of the Venturi effect driven by the high speed jet. Existence of optimal insertion characteristics as well as diffuser tipped cannula angle

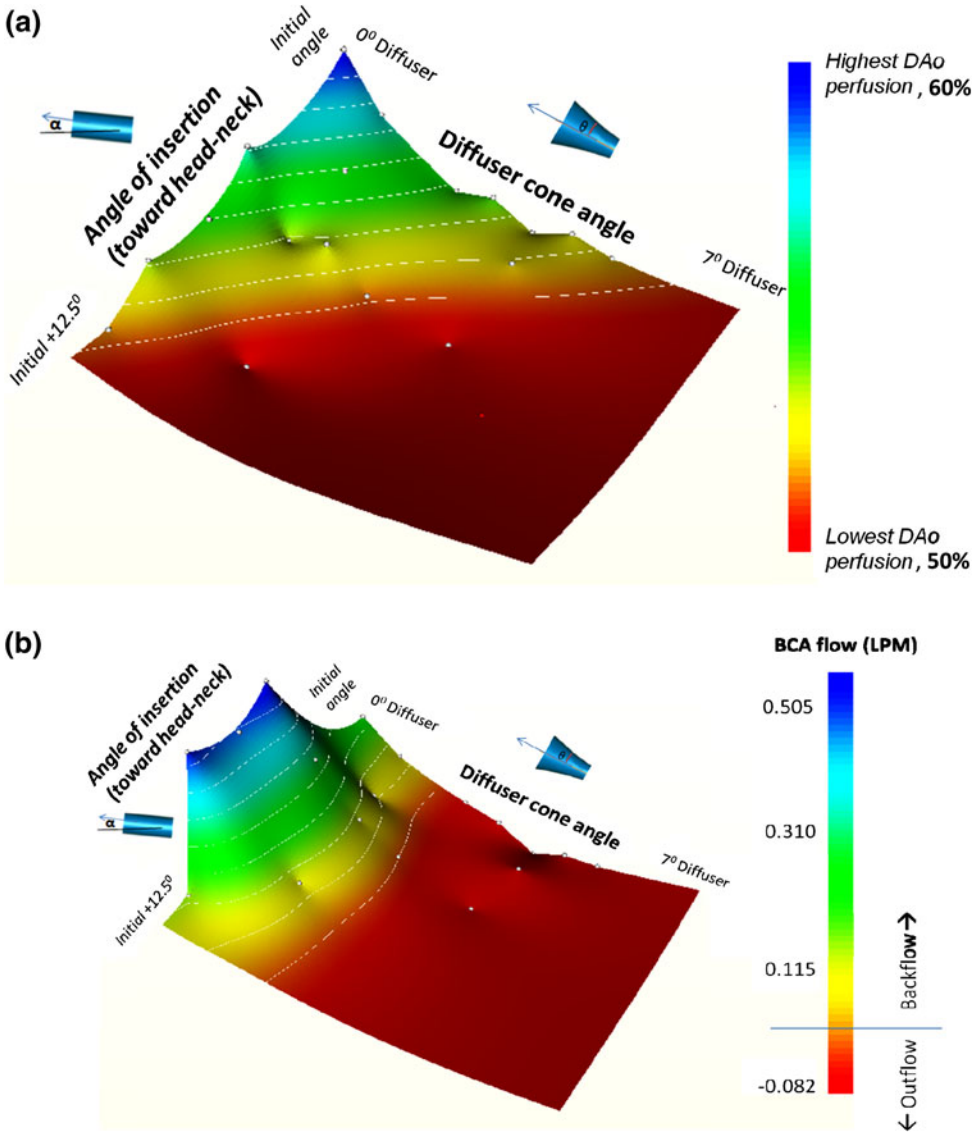

FIGURE 9. Shape sensitivity analysis results rendered as surface plots prepared by simple krigging. Expected variation of: (a) DAo perfusion; and (b) BCA flow for changes in insertion angle, α, relative to the baseline insertion configuration; and diffuser cone angle, θ, are indicated.

requires further investigation using a coupled inverse optimization framework.

DISCUSSION

Impact of Diffuser Design on Head–Neck Perfusion

The behavior of the aortic cannula jets proximal to the BCA ascribed to the Coanda-effect and the physics of the simple Venturi effect cumulatively provide an apt justification for poor perfusion of head–neck vessels of the aortic arch during high perfusion rates through tiny cannula apertures. These effects may be avoided by using a larger end-hole cannula angled toward the DAo; but cannula size is restricted on account of the small diameter of the pediatric aortic arch and the fact that aortic disruption must be kept to a minimum, while angulation of the tip too much away from the head–neck vessels may compromise cerebral perfusion, as confirmed by our analysis of orientation sensitivity of perfusion. On the other hand, a novel diffuser tipped cannula device not only reduced peak velocities and WSS observed in the aortic arch but also guaranteed positive perfusion for any given orientation of the tip. The altered hemodynamics due to either occlusion or backflow at the BCA can have repercussions on the direction of flow in the vertebral arteries, as has been revealed by previous clinical studies.[12] The effect of BCA backflow may be better understood in analogy to the condition of right subclavian steal

caused by brachiocephalic occlusion. This condition leads to antegrade flow in left vertebral artery and retrograde in right vertebral artery and compensation of BCA flow by both the subclavian artery and collateral antegrade flow supply to right common carotid artery and compromised cerebral blood flow (see Fig. 8). This situation is clearly undesirable and may be averted by virtue of the diffuser tipped aortic cannula as per this study.

In regard to the optimal diffuser design, the analytical solution to Jeffery Hamel wedge flow (White, Viscous fluid flow[42]) indicates a direct proportionality between the likelihood of flow separation at a given length in the direction of flow of a diverging channel, flow *Re* as well as diffuser cone angle, θ. Therefore, flow reversal leading to energy dissipation in the diffuser cone is likely to increase with both *Re* and θ, having a limiting case of corresponding to a velocity profile associated with vanishing WSS. Studies have also shown that the separation length is a function of θ,[20] indicating that at a higher *Re*, a smaller cone angle is desirable to remain in the flow regime of un-stalled flows which are merely decelerated by the diffuser. Further, for a large cone angle, a shorter length is desirable in order to mitigate the event of flow separation by along the length of the diffuser cone itself, corresponding to a velocity profile with vanishing WSS. This suggests the existence of a tradeoff between diffuser cone length and cone angle to prevent flow separation along the diffuser cone, which may also present itself as a solution to the issue of increased local energy dissipation and the Coanda effect documented previously in the aortic cannula design literature.[14,23] Further computational optimization studies may still need to be conducted in order to engineer the ideal diffuser tip investigating the effect of linear gradient in the walls in contrast with a hyperbolic or parabolic variation in the diffuser gradient.

The Swirl Inducer Design

In addition to the diffuser cone angle concept, a four-lobe swirl inducer design was also proposed to precede outflow of the cannula tip which is demonstrated in this study to help in improving coherence of the jet, delay onset of turbulence in the flow field, and also improve pressure-flow characteristics. Not only does the swirl inducer have benefits in terms of pressure-flow dynamics that may positively impact the operation of the extracorporeal circuit, but it helps accentuate a natural helical flow characteristic of blood vessels. The swirl inducer inherently creates helical flow which is established in the literature to constitutes an important flow signature in vessels.[29] In fact, recent literature has indicated that helical flow in the aortic arch, originated by its complex curvature amongst other complex anatomical traits,[9,19] plays a key role in promoting physiologically advantageous phenomena such as improved vascular washout and relatively uniform WSS distributions[28] as well as avoidance of turbulence development.[30] Given that aortic arches cannulated using today's state-of-the-art end-hole type cannulae are associated with a highly non-physiological flow fields, the design of outflow tips which facilitate physiologic helical aortic flows is of the essence.[5] Therefore, the swirl inducer may be a crucial design feature to investigate in future as a direction towards making aortic cannulation hemodynamics more physiological, holding promise for improving patient outcomes after CPB. In this study, the shape-sensitivity studies were limited to the diffuser cone alone but the swirl inducer design requires further investigation to determine its optimal features (i.e., number of turns, pitch and lobe shape).

Study Limitations and Future Direction

There are limitations to this study's numerical approach to modeling shape sensitivity of perfusion, despite the use of resistance boundary conditions. Other numerical studies have shown that cerebral blood flow results are less dependent on the cannula position if cerebral pressure autoregulation is assumed.[17] However, the present study considers fixed outflow resistances and ignores effects of cerebral autoregulation under the assumption that the drastic change in perfusion pressure and flow from a physiological to CPB scenario is too large to be compensated by autoregulation.[18] The time dependency of cerebral autoregulation cannot be completely discounted however and it may be possible to truly capture this effect using a more realistic approach to outflow resistance modeling that is capable of capturing the transition from physiological to CPB perfusion in a time-dependent fashion.

More generally, the cannula tip design concepts described in this study are applicable additionally to pediatric Ventricular Assist Devices (VADs). VADs have undergone decades of development and in recent years have gained increasing clinical use. The pumps themselves have evolved considerably but unfortunately there has been virtually no concerted attention in regard to cannulae. Consequently, the cannulae that are currently implanted in patients of all ages are rather primitive compared to the elegant blood pumps to which they are attached. In order to translate the diffuser tipped aortic cannula for use in conjunction with VADs or in CPB procedures on real patients, innovative introducers for the proposed diffuser-tip will require to be designed to enable minimum aortic

disruption while ensuring efficient, adequate and safe connection to the arterial circulation.

Finally, aortic cannulation may not be the only reason for neurological complications in neonates or pediatric patients. Clinical studies have suggested several aspects of patient management before and after the circulatory arrest (i.e., during low-flow CPB) that are as important in protecting the patient, including hemodynamic factors like flow pulsatility, thermal factors like adequate cooling of the brain, cold reperfusion and re-warming time,[37] as well as clinical factors that predispose neurological risk during CPB, like perioperative glucose levels.[13] While inferences in regard to these factors is difficult to obtain from retrospective studies and randomized clinical trials may help unravel some of these mysteries, lack of uniformity of in equipment and clinical practice makes data collection for CPB procedures in different institutions practically difficult. However, improvement in medical device technology such as by way of aortic cannula redesign as proposed in this study may help eliminate at least equipment-related factors in the complex series of events potentially impacting peri- and post-operative neurological complications.

CONCLUSION

Appropriate aortic cannulation today may be regarded an art more than a precise science without real time image-guidance feedback during the procedure and often precise orientation and depth of insertion is difficult in real CPB scenarios. In this study, CFD was employed to delineate the significant role of cannula tip design and orientation on head–neck perfusion during CPB as well as to help better define the science of appropriate aortic cannulation through analysis of head–neck perfusion in the aortic arch. The studies have revealed that aortic cannulation by an end-hole cannula tip is likely to lead to backflow from the BCA given the close-range Venturi effect of the high speed cannula jet stream. While the aortic orientation angle of the cannula tip was found to have a crucial role in determining the net head–neck flow volume, the issue of backflow at the BCA could not be averted by orientation alone. However, a net positive BCA outflow was possible to achieve only by altering the outflow tip to include a diffuser cone angle. More than orientation angle therefore, altering the end-hole tip design to a diffuser cone was found to play the most significant role improving head–neck perfusion. Placing the cannula sufficiently distanced from the BCA branch may also be critical in mitigating BCA backflow although such practice deviates from the conventional rule of thumb for positioning the aortic cannula ideally high up in the ascending aorta.[10]

Hence, overshadowing the rationale of lower outflow velocities, jet wake hemodynamics and sub-lethal blood damage presented in our earlier studies,[25] the diffuser tip presents itself as a promising new design avenue to explore in regard to aortic cannulae designed for neuroprotection during neonatal or pediatric CPB. This design also has potential application in adult aortic cannulae used in conjunction with CPB or VADs, where atheroembolism from the ascending aorta owing to cannula jets is a major cause for complications. The diffuser tipped cannula's reduced outflow velocities and therefore subdued reaction loads as well as WSS on the aortic wall may potentially mitigate the dislodgement of potentially mortal emboli created from atherosclerotic plaque. For future improvement of arterial cannula tip design, sensitivity of the proposed four-lobe swirl inducer design on pressure-flow characteristics and *in silco* cannulated aortic arch perfusion demands more critical attention. Based on flow visualization and pressure-flow characterizations presented in this work, future efforts must not only focus on characterizing effects of swirl lobe shape (i.e., groove depth), but also the pitch, number of turns and the diameter of the swirl inducer on the quality of the resulting cannula jet.

The described methodology for shape-sensitivity coupled CFD has great potential value in conducting patient-specific pre-surgical planning for medical device use. The identical methodology may be used to iteratively modify a parametrically defined cannula tip configuration (e.g., diffuser tip angle) within a gradient-based steepest descent optimization framework, and define optimal tip design on a patient-specific basis prior to surgery. It also lays a foundation for rapid evaluation of hemodynamic merit of several device designs in the context of vascular access device research and development.

ACKNOWLEDGMENTS

The study was supported through the Dowd-ICES fellowship award (2011–2012). We acknowledge Nikola Teslovich for assisting with use of the high-speed camera and pressure-flow measurement equipment. We also acknowledge the support of Taylor Newill from Optimal Solutions Software, LLC for his inputs regarding cannula tip geometry parameterization for the shape sensitivity analysis presented in this study.

REFERENCES

[1]Alemu, Y., G. Girdhar, M. Xenos, J. Sheriff, J. Jesty, *et al*. Design optimization of a mechanical heart valve for reducing valve thrombogenicity—a case study with ATS valve. *ASAIO J*. 56:389–396, 2010.

[2]Andropoulos, D. B., K. M. Brady, R. B. Easley, and C. D. Fraser, Jr. Neuroprotection in pediatric cardiac surgery: what is on the horizon? *Prog. Pediatr. Cardiol*. 29:113–122, 2010.

[3]Antaki, J. F., O. Ghattas, G. W. Burgreen, and B. He. Computational flow optimization of rotary blood pump components. *Artif. Organs* 19:608–615, 1995.

[4]Beerbaum, P., H. Korperich, J. Gieseke, P. Barth, M. Peuster, *et al*. Blood flow quantification in adults by phase-contrast MRI combined with SENSE—a validation study. *J. Cardiovasc. Magn. Reson*. 7:361–369, 2005.

[5]Brown, A. G., Y. Shi, A. Arndt, J. Müller, P. Lawford, and D. R. Hose. Importance of realistic LVAD profiles for assisted aortic simulations: evaluation of optimal outflow anastomosis locations. *Comput. Methods Biomech. Biomed. Eng*. 15(6):669–680, 2012.

[6]De Wachter, D., F. De Somer, and P. Verdonck. Hemodynamic comparison of two different pediatric aortic cannulas. *Int. J. Artif. Organs* 25:867–874, 2002.

[7]Dur, O., S. T. Coskun, K. O. Coskun, D. Frakes, L. B. Kara, *et al*. Computer-aided patient-specific coronary artery graft design improvements using CFD coupled shape optimizer. *Cardiovasc. Eng. Technol*. 2:35–47, 2011.

[8]Fallon, P., J. M. Aparicio, M. J. Elliott, and F. J. Kirkham. Incidence of neurological complications of surgery for congenital heart disease. *Arch. Dis. Child*. 72:418–422, 1995.

[9]Frydrychowicz, A., A. Berger, A. Munoz Del Rio, M. F. Russe, J. Bock, *et al*. Interdependencies of aortic arch secondary flow patterns, geometry, and age analysed by 4-dimensional phase contrast magnetic resonance imaging at 3 Tesla. *Eur. Radiol*. 22:1122–1130, 2012.

[10]Garcia-Rinaldi, R., G. D. Vaughan, 3rd, J. M. Revuelta, J. J. Goiti, and C. Gomez-Duran. Simplified aortic cannulation. *Ann. Thorac. Surg*. 36:226–227, 1983.

[11]Gundert, T. J., A. L. Marsden, W. Yang, and J. F. LaDisa, Jr. Optimization of cardiovascular stent design using computational fluid dynamics. *J. Biomech. Eng*. 134:011002, 2012.

[12]Horrow, M. M., and J. Stassi. Sonography of the vertebral arteries: a window to disease of the proximal great vessels. *AJR Am. J. Roentgenol*. 177:53–59, 2001.

[13]Huang, X. Z., H. Wang, H. Z. Xu, M. Ye, P. Jiang, *et al*. Association between perioperative glucose levels and adverse outcomes in infants receiving open-heart surgery with cardiopulmonary bypass for congenital heart disease. *Anaesth. Intensive Care* 40:789–794, 2012.

[14]Joubert-Hubner, E., A. Gerdes, P. Klapproth, K. Esders, J. Prosch, *et al*. An in vitro evaluation of aortic arch vessel perfusion characteristics comparing single versus multiple stream aortic cannulae. *Eur. J. Cardiothorac. Surg*. 15:359–364, 1999.

[15]Kaufmann, T. A., M. Hormes, M. Laumen, D. L. Timms, T. Linde, *et al*. The impact of aortic/subclavian outflow cannulation for cardiopulmonary bypass and cardiac support: a computational fluid dynamics study. *Artif. Organs* 33:727–732, 2009.

[16]Kaufmann, T. A., M. Hormes, M. Laumen, D. L. Timms, T. Schmitz-Rode, *et al*. Flow distribution during cardiopulmonary bypass in dependency on the outflow cannula positioning. *Artif. Organs* 33:988–992, 2009.

[17]Kaufmann, T. A., T. Schmitz-Rode, and U. Steinseifer. Implementation of cerebral autoregulation into computational fluid dynamics studies of cardiopulmonary bypass. *Artif. Organs* 36:754–758, 2012.

[18]Khuri, S. F., R. K. Brawley, J. B. O'Riordan, J. S. Donahoo, B. Pitt, *et al*. The effect of cardiopulmonary bypass perfusion pressure on myocardial gas tensions in the presence of coronary stenosis. *Ann. Thorac. Surg*. 20:661–670, 1975.

[19]Kilner, P. J., G. Z. Yang, R. H. Mohiaddin, D. N. Firmin, and D. B. Longmore. Helical and retrograde secondary flow patterns in the aortic arch studied by three-directional magnetic resonance velocity mapping. *Circulation* 88:2235–2247, 1993.

[20]King, P. I., M. E. Franke, and N. W. Martens. Effect of riblets on flow separation in a subsonic diffuser, La Jolla, CA, 9–12 July 1989, pp. 79–83.

[21]Kokotsakit, J., G. Lazopoulos, M. Milonakis, G. Athanasiadis, K. Romana, *et al*. Right axillary artery cannulation for surgical management of the hostile ascending aorta. *Tex. Heart Inst. J*. 32:189–193, 2005; discussion 185.

[22]Le, T. B., I. Borazjani, and F. Sotiropoulos. Pulsatile flow effects on the hemodynamics of intracranial aneurysms. *J. Biomech. Eng*. 132:111009, 2010.

[23]Magilligan, Jr., D. J., M. W. Eastland, W. A. Lell, J. A. DeWeese, and E. B. Mahoney. Decreased carotid flow with ascending aortic cannulation. *Circulation* 45:I130–I133, 1972.

[24]McElhinney, D. B., W. Tworetzky, and J. E. Lock. Current status of fetal cardiac intervention. *Circulation* 121:1256–1263, 2010.

[25]Menon, P. G., N. Teslovich, C. Y. Chen, A. Undar, and K. Pekkan. Characterization of neonatal aortic cannula jet flow regimes for improved cardiopulmonary bypass. *J. Biomech*. 26:00636–00637, 2012.

[26]Montoya, J. P., S. I. Merz, and R. H. Bartlett. A standardized system for describing flow/pressure relationships in vascular access devices. *ASAIO Trans*. 37:4–8, 1991.

[27]Moore, Jr., J. E., C. Xu, S. Glagov, C. K. Zarins, and D. N. Ku. Fluid wall shear stress measurements in a model of the human abdominal aorta: oscillatory behavior and relationship to atherosclerosis. *Atherosclerosis* 110(2):225–240, 1994.

[28]Morbiducci, U., R. Ponzini, D. Gallo, C. Bignardi, and G. Rizzo. Inflow boundary conditions for image-based computational hemodynamics: impact of idealized versus measured velocity profiles in the human aorta. *J. Biomech*. 46:102–109, 2013.

[29]Morbiducci, U., R. Ponzini, M. Grigioni, and A. Redaelli. Helical flow as fluid dynamic signature for atherogenesis risk in aortocoronary bypass. A numeric study. *J. Biomech*. 40(3):519–534, 2007.

[30]Morbiducci, U., R. Ponzini, G. Rizzo, M. Cadioli, A. Esposito, *et al*. Mechanistic insight into the physiological relevance of helical blood flow in the human aorta: an in vivo study. *Biomech. Model. Mechanobiol*. 10:339–355, 2011.

[31]Osorio, A. F., R. Osorio, A. Ceballos, R. Tran, W. Clark, *et al*. Computational fluid dynamics analysis of surgical adjustment of left ventricular assist device implantation to minimise stroke risk. *Comput. Methods Biomech. Biomed. Eng*. 16(6):622–638, 2011.

[32]Park, J.-S. Optimal Latin-hypercube designs for computer experiments. *J. Stat. Plan. Inference* 39:95–111, 1994.

[33]Payli, R., K. Pekkan, D. Zelicourt, D. Frakes, F. Sotiropoulos, *et al*. High performance clinical computing on the TeraGrid: patient-specific hemodynamic analysis and surgical planning. In: TeraGrid 2007 Conference Madison, WI, 2007.

[34]Pekkan, K., O. Dur, K. Sundareswaran, K. Kanter, M. Fogel, *et al*. Neonatal aortic arch hemodynamics and perfusion during cardiopulmonary bypass. *J. Biomech. Eng*. 130:061012, 2008.

[35]Pekkan, K., O. Dur, D. Zelicourt, R. Payli, F. Sotiropoulos, *et al*. Embryonic Intra-Cardiac Flow Fields at 3 Idealized Ventricular Morphologies. Milwaukee: APS, 2009.

[36]Polito, A., Z. Ricci, L. Di Chiara, C. Giorni, C. Iacoella, *et al*. Cerebral blood flow during cardiopulmonary bypass in pediatric cardiac surgery: the role of transcranial Doppler—a systematic review of the literature. *Cardiovasc. Ultrasound* 4:47, 2006.

[37]Pua, H. L., and B. Bissonnette. Cerebral physiology in paediatric cardiopulmonary bypass. *Can. J. Anaesth*. 45:960–978, 1998.

[38]Qiu, F., J. B. Clark, A. R. Kunselman, A. Undar, and J. L. Myers. Hemodynamic evaluation of arterial and venous cannulae performance in a simulated neonatal extracorporeal life support circuit. *Perfusion* 26:276–283, 2011.

[39]Svensson, L. G., E. H. Blackstone, J. Rajeswaran, J. F. Sabik, III, B. W. Lytle, *et al*. Does the arterial cannulation site for circulatory arrest influence stroke risk? *Ann. Thorac. Surg*. 78:1274–1284, 2004; discussion 1274–1284.

[40]Tokuda, Y., M. H. Song, Y. Ueda, A. Usui, T. Akita, *et al*. Three-dimensional numerical simulation of blood flow in the aortic arch during cardiopulmonary bypass. *Eur. J. Cardiothorac. Surg*. 33:164–167, 2008.

[41]Wang, Y., O. Dur, M. J. Patrick, J. P. Tinney, K. Tobita, *et al*. Aortic arch morphogenesis and flow modeling in the chick embryo. *Ann. Biomed. Eng*. 37:1069–1081, 2009.

[42]White, F. M. Viscous Fluid Flow. New York: McGraw-Hill, 1991.

[43]Wu, J., J. F. Antaki, T. A. Snyder, W. R. Wagner, H. S. Borovetz, *et al*. Design optimization of blood shearing instrument by computational fluid dynamics. *Artif. Organs* 29:482–489, 2005.

[44]Zhu, L., X. Zhang, and Z. Yao. Shape optimization of the diffuser blade of an axial blood pump by computational fluid dynamics. *Artif. Organs* 34:185–192, 2010.